

Cite this: *Mater. Adv.*, 2025,  
6, 5687

# Mid-Infrared monitoring of aromatic hydrocarbons in an aquatic environment based on polyhydroxyalkanoate biopolymers for use in a chalcogenide infrared microsensor

Martin Vrážel,<sup>a</sup> Duc Trung Tran,<sup>b</sup> Patrick Louergue,<sup>b</sup> Anthony Szymczyk,<sup>b</sup> Radwan Chahal,<sup>b</sup> Anthony Courtois,<sup>c</sup> Marek Bouška,<sup>a</sup> Joel Charrier,<sup>d</sup> Petr Němec <sup>a</sup> and Virginie Nazabal <sup>\*ab</sup>

In the context of mid-infrared monitoring of chemical pollutants in an aquatic environment, petrosourced polymers are typically used for the functionalization of optical infrared transducers. These polymers serve to extract pollutants from water solutions while minimizing the interference caused by the strong infrared absorption of water in the relevant spectral regions. This work explores the feasibility of replacing petrosourced polymers with their bio-based alternatives. The inspiration behind this study was to find durable and environmentally friendly polymer materials, capable of replacing conventional polymers, which are deposited on a chalcogenide infrared transducer designed for evanescent wave spectroscopy. Regarding the life cycle analysis of the optical infrared transducer, this substitution aims to minimize potential pollution arising from the manufacturing process, as well as its degradation or wear during field use. For this, polymers from the polyhydroxyalkanoate (PHA) family were considered and several commercial PHAs with different molecular structures were chosen for this evaluation. The optical transducers were functionalized by depositing a PHA membrane, which was prepared using a phase inversion procedure. Different solvents were evaluated for this process as well as two casting methods, namely spin-coating and knife-coating. The two least crystalline PHA samples (crystallinity degree of 0% and 19%) were found to be suitable for BTX detection, unlike other tested variants of PHAs. Calibration curves were then established with these two polymers, followed by a regeneration experiment, where the amorphous PHA demonstrated the ability to be regenerated by distilled water under ambient conditions. This paper presents, for the first time, the use of a bio-based polymer for mid-infrared *in situ* monitoring of aromatic hydrocarbons in aquatic environments. Furthermore, these polymers are compatible with infrared microsensors based on chalcogenide materials. These results open up possibilities for the use of PHAs in a new field, where their application has been previously unexplored and propose an environmentally friendly solution to the problem of water absorption.

Received 13th January 2025,  
Accepted 27th May 2025

DOI: 10.1039/d5ma00033e

rsc.li/materials-advances

## Introduction

For the last few decades, the pollution of the environment and aquatic systems has increased due to intensive urbanization and industrialization.<sup>1,2</sup> This rapid progress of pollution poses a significant threat to both freshwater and marine ecosystems, due to its toxic effects, which lead to severe degradation of

fauna and flora. Despite the growing awareness of the issue and efforts to decrease the amount of pollutants present in the aquatic environment, hydrocarbon pollutants continue to affect the environment, originating from both man-made and natural sources. As the whole world relies on clean water for both industry and consumption, several techniques have been developed to monitor and ensure the quality of aquatic environments.<sup>3–6</sup> Techniques for monitoring the quality of water sources are chosen based on the location where the measurements are taking place, with a recent focus on *in situ* monitoring stations. Traditionally, monitoring was conducted through *ex situ* laboratory analysis (*e.g.* headspace gas chromatography, gas chromatography combined with mass spectrometry, high-performance liquid chromatography). This process

<sup>a</sup> Department of Graphic Arts and Photophysics, Faculty of Chemical Technology, University of Pardubice, Studentska 573, 53210 Pardubice, Czech Republic<sup>b</sup> Univ Rennes, CNRS, ISCR – UMR6226, F-35000 Rennes, France.  
E-mail: virginie.nazabal@univ-rennes.fr<sup>c</sup> Polymaris Biotechnology, 160 rue Pierre Rivoalon, 29200 BREST, France<sup>d</sup> Univ Rennes, CNRS, Institut Foton – UMR 6082, F-22305 Lannion, France

requires field sampling, transportation of samples, and subsequent laboratory measurements. These methods are typically expensive, time-consuming, and pose a risk of inaccuracy. This risk arises because water samples can undergo chemical changes or become contaminated as a result of physical, chemical or biological reactions during the interval between sampling and analysis. For these reasons, recent efforts have focused on portable microfluidic optical infrared sensors, based on evanescent wave spectroscopy, which are placed directly in contact with the sample, allowing for *in situ* analysis. This technique exhibits improved sensitivity and selectivity towards chemical pollutants. However, other important factors such as portability, versatility, ease-of-use and cost reduction are still a subject of development.<sup>5,7–11</sup> Furthermore, despite achieving results comparable to laboratory methods (with detection limits up to  $\mu\text{g-ng L}^{-1}$ ), the ability of portable chemical sensors to identify a specific molecule in a mixture remains a significant challenge when analysing real environmental samples.<sup>3,4</sup>

In this study, benzene, toluene, and xylenes (BTX) were chosen as target pollutants for analysis, as they pose a serious threat to human health due to their carcinogenic properties. Their presence in the environment at potentially high concentrations can arise due to natural sources (crude oil, emission of forest fires) or as a consequence of human activities (engine emissions, oil processing, environmental disasters).<sup>12,13</sup>

While multiple *in situ* mid-infrared (MIR) techniques (*e.g.* IR spectroscopic ellipsometry, reflection absorption IR spectroscopy, ATR operating with Fourier-transform spectroscopy) with multiple geometries (such as simple reflection, transmission, and fiber waveguide) can be used as suitable techniques to detect a wide range of organic substances, evanescent wave spectroscopy was selected for this study. This method was chosen not only for its good sensitivity and selectivity, but also for its non-destructive measurement capability within the wavelength range between 4000 and 400  $\text{cm}^{-1}$  (2.5–25  $\mu\text{m}$ ).<sup>5,14</sup> Analytes near the surface of photonic waveguides interact with an evanescent field of infrared light, the latter penetrating a few micrometers into the medium containing the analytes. The compound-specific attenuation of the IR radiation results in discriminatory IR spectra comparable to conventional macroscopic IR-ATR spectroscopy.<sup>15</sup>

In general, the key components of any MIR sensor include: (i) a light source: MIR sensors typically employ tunable infrared sources, such as quantum cascade lasers (QCLs), interband cascade lasers (ICLs), MIR LEDs, or broadband emitters, to generate a continuous spectrum or a specific wavelength in the case of lasers; (ii) a transducer: an interface, where the analytes interact with the infrared light, producing specific spectral signatures absorption-based detection; (iii) a detector: to capture the intensity changes in the infrared spectrum after its interaction with the analyte; (iv) a signal processing unit: for analyzing the acquired spectra using computational tools to identify, quantify, and characterize the measured samples.<sup>16</sup>

Several material platforms are suitable to serve as transducers in MIR spectroscopy. The selected material has to be transparent in the MIR spectrum, with low absorption and a wide

transparency window. It should have a stable refractive index and low propagation losses at the chosen wavelengths. Commonly used materials include silicon, germanium, zinc selenide or a wide variety of chalcogenide glasses. These materials are employed in different waveguide configurations (*e.g.* ribbon, ridge or diffused) and with a variety of claddings (*e.g.*  $\text{SiO}_2$ , Si or air).<sup>17</sup>

The objective is to develop a microsensor with suitable selectivity and sensitivity to organic chemical molecules in the case of accidental pollution, using high MIR transparency of chalcogenide glass-based optical transducers. These transducers can be tailored to ideally meet the emission characteristics of the light source toward maximizing the signal-to-noise ratio during evanescent field absorption measurements. Their high transparency window includes the IR fingerprint signatures of fundamental vibrations of organic species and biomolecules ( $\lambda \geq 6.7 \mu\text{m}$  or  $\leq 1500 \text{ cm}^{-1}$ ), providing a simple, reliable, fast, and non-destructive method for detecting and determining their concentration in complex matrixes.<sup>2</sup> This was proven in the past for the analysis of water-free samples, where quantitative spectra of the samples were obtained by using a Beer–Lambert linear relation, and chalcogenide thin films were successfully employed for detecting organic pollutants or biomolecules.<sup>18</sup> However, in the case of aquatic samples, the functionalization of the optical transducer becomes necessary for extracting molecules from water to lower the negative influence of water absorption on IR measurements and to protect the surface of the sensor. This is typically achieved by depositing a polymer membrane on top of the sensor. Various types of polymers (*e.g.* polyisobutylene, poly(styrene–isoprene–styrene), and ethylene–propylene co-polymer)<sup>7–9</sup> were tested for the detection of aromatic hydrocarbons in aqueous solutions. However, all of these polymers are petroleum-based and thus contribute to the pressure exerted on fossil resources. In addition, these polymers may degrade upon contact with the environment and be released into the water over time. This study instead focuses on using bio-based polymers, aiming to use environmentally friendly materials that would not adversely affect their surroundings, even if they degrade.

Polymers from the polyhydroxyalkanoate (PHA) family were selected for this work due to their wide range of properties, which arise from their diverse molecular structures and compositions (Fig. 1a).<sup>19,20</sup> They are microbial biopolymers, produced from renewable resources and demonstrate excellent biocompatibility. PHAs are linear homo- and co-polyesters produced by bacterial fermentation and have versatile properties. As a result of the diverse production conditions, the PHA side chain length and composition can vary,<sup>21,22</sup> thus influencing the final thermomechanical properties of the macromolecule.<sup>23,24</sup>

The wide range of physicochemical and mechanical properties of native PHAs, combined with their biocompatibility and potential for modification through chemical and biological methods, has driven research into developing new PHAs with tailored properties for specific applications. As a result, PHAs are being applied in various fields of technology, including



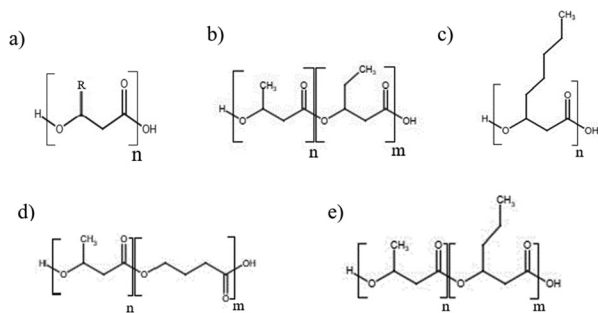


Fig. 1 Chemical structure of the used PHA polymers: (a) general structure of PHA; (b) P3HB3HV; (c) PHO; (d) P3HB4HB; (e) P3HB3HH.

medical implants, drug carriers, biofuels, packaging or membranes for water treatment and solvent–mixture separation.<sup>20,25–27</sup> They are emerging as sustainable alternatives to conventional petroleum-derived polymers, offering a more environmentally friendly option.

In this context, this study reports on the first application of PHAs for the functionalization of mid-infrared microsensors for BTX detection in water. For this application, a thin layer of PHA is to be deposited on top of a chalcogenide amorphous thin film, which will be used as an optical infrared transducer. Several commercially available PHAs were selected and evaluated for this application. Particular attention was paid to the influence of the PHA's physicochemical properties on the detection performance. As transport of a permeant through a dense polymer membrane in contact with a liquid is directly related to the solvent's affinity for the membrane and to the polymer film's nanostructure, this study focused on the surface properties (hydrophilicity/hydrophobicity) and crystallinity of the PHA-based membranes. PHA-based membranes were further evaluated for BTX detection by ATR-FTIR, and the results were compared, considering the varying properties of different PHAs.

To the best of our knowledge, the present study is the first one reporting on the use of bio-based polymers for the functionalization of optical sensors for monitoring aquatic pollution.

The MIR spectral range has recently attracted growing interest in biosensing and the food industry, owing to its potential for enabling customizable, highly reliable, and portable sensing solutions for on-site chemical analysis. These technologies offer accurate molecular detection and real-time monitoring. However, despite significant progress, water absorption remains a major challenge. Water exhibits strong absorption bands in the MIR region – particularly around 2.7, 3.0 and 6.1  $\mu\text{m}$ , which can severely interfere with the detection of other compounds by obscuring or overlapping with their spectral signatures. One common strategy to address this issue

is the use of membranes in the form of thin films, which can help reduce water interference and improve signal clarity. As stated above, PHAs have the potential to be fine-tuned towards extraction of specific types of molecules, making them a promising candidate for applications across several expanding industries. Multiple articles have now reported on the use of MIR spectroscopy for molecule detection; however, no solution to the problem of water absorption has been presented, other than using dry samples including the analytes or surface functionalization by petroleum-based polymers.<sup>15,16,28–30</sup>

## Experimental

### Chemicals

A stock solution of BTX was prepared by mixing benzene (99%), toluene (>99.5%), *o*-xylene (97%), *m*-xylene (>99%) and *p*-xylene (>99%), all obtained from Sigma-Aldrich and used as provided, to prepare a stock solution of a concentration of 50 000 ppm in methanol (anhydrous, >99.8%, Sigma-Aldrich). To obtain aqueous solutions of the chosen concentrations, an appropriate amount of stock solution was mixed with distilled water. Four PHA variants were sourced from three producers (Table 1), and their structure can be seen in Fig. 1. All selected PHAs (except PHO) were copolymers of hydroxybutyrate monomer and differ in the structure of the comonomer. All PHAs were used as provided.

For dissolving the polymers, different solvents were tested, namely: chloroform (anhydrous,  $\geq 99.8\%$ , Sigma-Aldrich), Rhodiasolv Polarclean ( $\geq 98\%$ , Solvay), cyrene ( $\geq 98.5\%$ , Sigma-Aldrich) and dichloromethane ( $\geq 99.5\%$ , Sigma-Aldrich).

### Membrane fabrication

Membrane formation was induced by a phase inversion procedure involving three steps: (i) polymer dissolution into a solvent, (ii) casting of the solution on a substrate and (iii) precipitation of the membrane by phase inversion induced by solvent evaporation.

The desired amount of polymer was first dissolved in the required amount of solvent and mixed at a fixed temperature (Table 2) until the polymer was completely dissolved. Prior to deposition, the solutions were put into an ultrasound bath for 15 min to remove any air bubbles.

Four materials were chosen as substrates for deposition: microscopic glass (for preliminary tests), silicon wafer (for atomic-force microscopy and contact angle measurements), chalcogenide glass (of Ge–Sb–Se composition) deposited on silicon wafer (for scanning electron microscope measurement) and a ZnSe prism (for IR measurements). The reason behind

Table 1 Types of PHAs used in this study

Polymer	Referred to as (in this work)	Commercial name	Producer
Poly(3-hydroxybutyrate- <i>co</i> -3-hydroxyvalerate)	P3HB3HV	BioseaLite	Polymaris biotechnology (France)
Poly(3-hydroxybutyrate- <i>co</i> -3-hydroxyoctanoate)	PHO	—	Polymaris biotechnology (France)
Poly(3-hydroxybutyrate- <i>co</i> -4-hydroxybutyrate)	P3HB4HB	PHACT A1000P	CJ biomaterials (South Korea)
Poly(3-hydroxybutyrate- <i>co</i> -3-hydroxyhexanoate)	P3HB3HH	PHA BP 350-05	Bluepha Microbiology technology (China)



Table 2 Description of the finalized combinations between PHA polymers and solvents, with deposition done by drop-coating

Polymer	Solvent	Solubilisation temperature (°C)	Time dissolve (min)	Concentration for deposition (% w/w)	Observed properties of the film
P3HB3HV	Chloroform	50	20	10	Porous, poor adhesion
	Cyrene	60	40	10	Fragile, porous
	Polarclean	80	40	10	Very soft, easily damaged
	Dichlormethane	37	20	10	Homogenous, good adhesion
P3HB3HH	Dichlormethane	37	20	10	Homogenous, good adhesion
P3HB4HB	Dichlormethane	37	60	10	Homogenous, very good adhesion
PHO	Dichlormethane	25	10	20	Homogenous, good adhesion

choosing chalcogenide glass was for the future development of an optical sensor based on a chalcogenide waveguide and polymer membrane. The chalcogenide glass will serve as a guiding layer of the prepared optical waveguide, as mentioned above. Zinc selenide ATR crystals (80 mm × 10 mm × 4 mm; made by Innovation Photonics), with an angle of incidence of 45° were used as a testing ground for ATR experiments with the polymers.

For the deposition of the polymer solution on a substrate, three techniques were evaluated. The first was drop-coating, which is a simple method consisting of pouring the solution on top of the substrate and letting the solvent evaporate. This method generally does not produce thin films, and the results are not easy to reproduce, but the method served well as a preliminary test. The second method of deposition was spin-coating, which uses centrifugal force to spread the dropped solution evenly on the surface of a target. This method is capable of producing thin films and has high reproducibility, as the thickness of the prepared film is governed by the viscosity of the solution, the rotational speed of the machine, the duration of spin-coating and the volume of solution deposited on the target. The third tested method was knife-coating, where an excess of coating material is applied to the substrate and removed by an adjustable blade to achieve the desired thickness of coating. This method is also capable of producing thin films and has high reproducibility. The thickness of the film is determined by the height of the knife and the speed at which the knife is moving, as well as the solution viscosity. Spin-coating and knife-coating were, to our knowledge, used for the first time for depositing polymers of the PHA family onto planar waveguides.

The thickness of the deposited polymer significantly impacts the sensor's properties (a thicker film increases the measurement time but provides stronger signals). Therefore, it must be carefully selected based on the depth of penetration of the evanescent wave, which is directly influenced by the wavelength of the radiation and the refractive indices of both the prism and the polymer film. This penetration depth can then be used to determine the appropriate film thickness, which needs to be greater than the depth of the evanescent wave penetration:<sup>31</sup>

$$d_p = \frac{\lambda}{2\pi n_1 \left( \left( \sin^2 \theta - \frac{n_2}{n_1} \right)^2 \right)^{\frac{1}{2}}} \quad (1)$$

where  $\lambda$  is the wavelength of the incident light,  $n_1$  and  $n_2$  are the refractive indices of the prism and the polymer, respectively, at

this wavelength, and  $\theta$  is the angle of incidence. This formula suggests a penetration depth of approximately 2 to 3  $\mu\text{m}$  for the spectral region, corresponding to the fingerprints of the organic molecules (650 to 900  $\text{cm}^{-1}$ ). To avoid the absorption tail of the evanescent wave being absorbed by the water, the film is preferably prepared with a thickness about three times greater than the penetration depth.<sup>31</sup> Therefore, to achieve a balance between optimal polymer film thickness and good response time, 5  $\mu\text{m}$ -thick films were chosen for the ATR measurements in this study.

As the functionalization of a sensor by a polymer membrane requires the preparation of a PHA solution, an appropriate solvent had to be found. Halogenated organic solvents are well known as excellent candidates for this application.<sup>26,27</sup> However, recent years have seen a shift towards new, greener solvents as substitutes to minimize exposure to the toxicity associated with halogenated compounds. For this reason, in this study, two halogenated solvents (chloroform and dichloromethane) and two green, harmless solvents (Rhodiasolv Polarclean and Cyrene) were considered for membrane preparation (Table 2). P3HB3HV served as a testing polymer for all of the used solvents, with the prepared concentrations ranging from 10% to 20% w/w. However, no significant changes were observed and, as such, 10% was chosen as the optimal solution viscosity for all film preparation methods (except for PHO where a 20% solution was used to increase the viscosity).

For knife-coating, experiments were carried out using a thermostatic automatic casting machine (Elcometer 4340). The casting height was set to an appropriate value and the casting speed to 4  $\text{cm s}^{-1}$ . All the tools (casting machine, casting knife, supports for the substrate) were heated to temperatures below the solubilisation temperature of the solvent used (Table 2). After the deposition, the film was left on the casting machine for five minutes and then removed and left under the hood for 1 h at room temperature for complete solvent evaporation.

For spin-coating, the experiments were carried out on a spin-coater (WS-400B-6NPP-Lite Spin Processor by Laurell Technologies), under a nitrogen atmosphere. The prism was heated to a temperature below the solubilisation temperature of the used solvent, and 0.5 ml of solution was spread across the surface of a prism and spun for 30 s at 600 rpm to achieve a thickness of 5  $\mu\text{m}$ . The substrate was then removed from the machine and the film was left to dry under a hood for 1 h at room temperature. Unlike for knife-coating, this setup did not allow for continuous heating of the substrate and other equipment.



### Polymer and membrane characterization

Monomeric compositions of the different PHAs were obtained by proton nuclear magnetic resonance ( $^1\text{H}$  NMR, Bruker 400 MHz), when the content (in mol%) of the copolymers was found by comparing the integrations of the appropriate peaks in the NMR spectra.

The molecular weight of the PHAs was determined by size exclusion chromatography (SEC), using three successive columns ( $2 \times$  ResiPore and  $1 \times$  PL gel Mixed C from Agilent) and a Waters UV detector working at a wavelength of 241 nm. The eluent was chloroform (for P3HB4HB, P3HB3HH and P3HB3HV) and tetrahydrofuran (for PHO) with a flow rate of  $0.8 \text{ mL min}^{-1}$ . Polystyrene standards were used for calibration.

The crystallinity of the used polymers was determined by differential scanning calorimetry (Q10 DSC, TA Instruments). The samples were heated in sealed aluminium pans from 20 to  $200 \text{ }^\circ\text{C}$  at a rate of  $10 \text{ }^\circ\text{C min}^{-1}$  under a  $40 \text{ mL min}^{-1}$  flow of nitrogen. The crystallinity ( $X_c$ ) of the PHAs was determined by comparing the melting enthalpy of the samples ( $\Delta H_m$ ) with the melting enthalpy of an ideal PHA crystal ( $\Delta H_m^0 = 146 \text{ J g}^{-1}$  for 100% crystallinity):

$$X_c (\%) = 100 \times (\Delta H_m / \Delta H_m^0) \quad (2)$$

The reproducibility of the prepared films (mainly their thickness) was determined by a profilometer (Tencor P-7 Stylus Profiler). This involved creating a step in the film and measuring its height at multiple points using a stylus tip, reconstructing the topography from the changes along the  $Z$  axis.

To ascertain the adhesion between the polymer and chalcogenide glass and to observe the microstructure of the film, scanning electron microscopy (SEM) was utilized to analyse the cross section of the film deposited on silicon wafer. The used equipment (JEOL JSM 7100 F) was operated at 5–8.5 mm working distance, with an accelerating voltage of 10 kV. As all PHA polymers would be sheared off during the wafer breakage under ambient conditions, the polymer had to be frozen under liquid nitrogen and the wafer carefully broken in the place of interest. For PHAs with high crystalline content, this method often resulted in the film peeling off the wafer, which required a careful manipulation.

The topography of the deposited films was measured by amplitude modulated atomic-force microscopy (AFM, Solver Next, NT-MDT). Tapping mode imaging was used on an area of  $5 \mu\text{m} \times 5 \mu\text{m}$  and  $10 \mu\text{m} \times 10 \mu\text{m}$  with the rate of scan being one line per 2 s, and the whole image consisted of 512 lines. root mean square (RMS) values were used for analysing the surface roughness.

The hydrophobicity of the deposited films was evaluated by contact angle measurements. A series of measurements were conducted on a contact angle goniometer (OCA 50EC, DataPhysics Instruments) using a static sessile drop method, which consists of depositing a droplet of distilled water on the researched surface and capturing an image of a liquid–solid interface. The obtained image is then analysed, and the angle between the water and surface is measured by fitting to the Ellipse model. The volume of

deposited droplets was in the range from 1.5 to  $1.8 \mu\text{L}$ , while the temperature in the room was set to  $20 \text{ }^\circ\text{C}$ . The measurement immediately started after the droplet's deposition and in the interval of 10 s, 14 images were taken. After that, each image was fitted, and the average value was calculated. Five measurements were done on different locations for each polymer.

### ATR-FTIR spectrometry measurement of BTX molecules

ATR-FTIR spectrometry measurements were performed on a Nicolet Fourier-transform infrared spectrometer (iS50 Spectrometer by ThermoFischer), equipped with an ATR accessory (HATR produced by PIKE technologies). The flow cell (with the chamber volume of  $500 \mu\text{L}$ ), containing ZnSe crystals coated by PHA film, was installed onto the accessory, and the tested solution was pumped across the surface with a peristaltic pump at a flow rate of  $3 \text{ mL min}^{-1}$ . Given the inner geometry of the chamber, the velocity was calculated to be  $0.007 \text{ m s}^{-1}$ .

The infrared spectra of the molecules of benzene, toluene and the three isomers of xylene include numerous characteristic absorbance bands between  $650$  and  $3100 \text{ cm}^{-1}$ . The strongest signal is observed in the range between  $650$  and  $900 \text{ cm}^{-1}$ ,<sup>32</sup> where it is possible to distinguish individual molecules. The second ( $950$ – $1200 \text{ cm}^{-1}$ ) and third ( $1450$ – $1650 \text{ cm}^{-1}$ ) regions<sup>32</sup> can also be exploited for detecting BTX molecules, though a significant drop in the strength of the signal is to be expected. Because of that, attention was mainly focused on the first area. The characteristic absorption bands chosen for the detection of BTX using ATR-FTIR spectrometry are located at  $674 \text{ cm}^{-1}$  for benzene,  $692$  and  $727 \text{ cm}^{-1}$  for toluene,  $741 \text{ cm}^{-1}$  for *o*-xylene,  $690$  and  $767 \text{ cm}^{-1}$  for *m*-xylene and  $794 \text{ cm}^{-1}$  for *p*-xylene.<sup>32,33</sup> Importantly, the absorption band at  $690 \text{ cm}^{-1}$  for *m*-xylene overlaps with the band of toluene at  $692 \text{ cm}^{-1}$ , causing the bands to appear as one and effectively doubling the size of the band at that position. To align the present results with previous studies, the absorbance band at  $692 \text{ cm}^{-1}$  was marked as toluene M-X.<sup>33</sup>

For all spectra, the PHA-coated ZnSe crystal was used as a background. The absorbance band intensities were analysed using OriginLab (version 2022, OriginLab, Northampton, MA, USA). The procedure consisted of manually integrating the bands. The baseline was set by the User Defined method, while individual anchor points were detected by the 2nd derivative (zeroes) method, utilising the fact that the baseline area has a smaller curvature than the absorbance band. After the adjacent-averaging smoothing, the second derivative at each point is calculated. All data points whose second derivative approaches zero (under the tolerance) are used to make a second-order polynomial fit. With the fitted baseline in hand, the points closest to the fitted line were selected as anchor points and interpolated to generate a line. This process creates a baseline, which makes it possible to manually select absorbance band areas and integrate them for calculation.

While measurements were being made on the ATR-FTIR spectrometer, another series of parallel measurements was carried out on a gas chromatograph combined with mass spectrometry (GC-MS 7890A system from Agilent Technologies).



The aim was to determine the actual concentration of the solutions using GC–MS to establish a validated calibration curve for the ATR-FTIR spectrometry. It was also necessary to determine the time period during which the BTX solutions prepared could be used without any change in concentration, given the high volatility of the molecules. The measured periods were one and two weeks for the stock solution of 50 000 ppm, 2 h for the daughter solution of 2500 ppm, and 90 min for the solution of 1 ppm, corresponding to the ATR-FTIR analysis time in the latter case. The results showed that the 1 ppm and 2500 ppm solutions maintained the required concentration during the time frames tested. Surprisingly, the stock solution, which was kept at 4 °C after preparation, also showed no significant decrease in concentration over the period of two weeks. Despite that, as a precautionary measure, the stock solution was renewed at the beginning of each week, to ensure reproducibility of the results.

## Results and discussion

As the PHA membranes are being tested as potential films for forming a surface of the optical waveguide in the making, they were characterised for their sensitivity towards aromatic hydrocarbons and also for their reproducibility and reusability. As the PHAs had not previously been used in this context, particular attention was also paid to other film properties.

Table 3 describes additional properties of the tested polymers, namely their copolymer content (measured by NMR), crystallinity (measured by DSC), molecular weight (measured by SEC), melting point (by DSC), glass transition temperature (provided by the manufacturer) and contact angle (by sessile drop measurement).

The copolymer content was 30% for P3HB4HB, 14% for P3HB3HV, 10% for P3HB3HH and 0% for PHO. The polymers differed greatly regarding their crystallinity. Three polymers were semi-crystalline, containing both amorphous (disordered) and crystalline (ordered) regions. These polymers (with their crystallinity percentage) were P3HB3HV (43%), P3HB3HH (27%) and PHO (19%). The P3HB4HB polymer (0%) was amorphous (with a predominantly disordered structure). This distribution allowed for direct comparison between the polymers based on their crystallinity, to evaluate this property in regard to infrared measurements.

The molecular weights of the tested polymers increased in the following order: PHO < P3HB3HH < P3HB3HV < P3HB4HB. Although their molecular weights are relatively high compared to low-molecular-weight polymers, the tested PHAs had lower molecular weights than other polymers previously used for infrared pollutant detection in water.<sup>7</sup> The glass

transition temperatures were below the room temperature and thus could not be observed in the obtained DSC curves. For the intended application of polymers in water, it is generally preferable for polymers to be used in environments above their glass transition temperature, where the polymer chains have increased segmental mobility and free volume, facilitating the diffusion and partitioning of molecules.

Contact angle measurements performed on polymer thin films deposited on silicon wafers gave values of  $67 \pm 3^\circ$  for P3HB3HV,  $76 \pm 1^\circ$  for P3HB3HH and  $79 \pm 3^\circ$  for P3HB4HB, indicating that these PHA films can be considered as slightly hydrophilic (as the contact angle is slightly below  $90^\circ$ ). Conversely, PHO was found to be slightly hydrophobic with a contact angle value of  $102 \pm 1^\circ$ . These data are in line with some studies reporting that the contact angle values of untreated PHA films are in the range of  $60$ – $85^\circ$  degrees for P3HB copolymers and in the range of  $100$ – $105^\circ$  for PHO films.<sup>27,34,35</sup>

The properties mentioned above can be compared to other previously reported polymers used for BTX detection in water. For example, polyisobutylene—a petroleum-based amorphous polymer, with a molecular weight of 500 kDa, a glass transition temperature at  $-64^\circ\text{C}$  and a contact angle of  $110.1^\circ \pm 2.9^\circ$  (ref. 36)—was successfully employed as a membrane for BTX measurements. Its properties are comparable to those observed for the PHAs studied here.

### Fabrication of the PHA-based membrane and assessment of its compatibility with a chalcogenide infrared microsensor

A variety of solvents were evaluated for preparing polymer solutions (Table 2).

For both halogenated solvents, total dissolution of the P3HB3HV was observed after 20 min, but dichloromethane required a lower temperature ( $37^\circ\text{C}$ ) compared to that of chloroform ( $50^\circ\text{C}$ ). This observation confirmed the efficiency and rapidity of PHA dissolution using halogenated solvents. Conversely, Rhodiasolv Polarclean and Cyrene also succeeded in dissolving P3HB3HV but at higher temperatures ( $80$  and  $60^\circ\text{C}$ , respectively) and after a considerable time (40 min) in comparison with halogenated solvents.

As P3HB3HV was used in the initial experiments, this polymer was also subjected to most extensive testing, including a broader selection of solvents and a wider range of concentrations.

The initial depositions were done by drop-coating the solutions of concentrations between  $10$ – $20\%$  on microscopic glass (pre-heated to below the solubilisation temperature) and then evaluated for their properties and resistance to be penetrated by water droplet. The observed properties can be found in Table 2

Table 3 Thermal, structural and surface properties of PHA polymers

Polymer	Copolymer content (mol%)	Crystallinity	$M_w$ (kDa)/polydispersity	Melting point ( $^\circ\text{C}$ )	Glass transition temperature	Contact angle ( $^\circ$ )
P3HB3HV	14% HV	43	330/4	173	NA	$67 \pm 3$
PHO	No copolymer	19	103/2	57	NA	$102 \pm 1$
P3HB4HB	30% HB	0	507/2	NA	$-15$	$79 \pm 3$
PHO	10% HH	27	265/5	104	$-2$	$76 \pm 1$



and matched the properties of films prepared by other techniques.

The results were as follows. While solutions utilizing chloroform as a solvent quickly created films, the adhesion to glass was very poor (the film peeled off the surface on its own) and a water droplet was able to penetrate the film, reaching the glass underneath. These results were obtained regardless of the concentration. Solutions prepared with Cyrene formed a very fragile film (could be damaged by a soft touch), and while the adhesion to the glass was good, it was also quickly penetrated by water. Higher concentration did not change its behaviour. For films prepared by Polarclean, the film resulted in a very soft, fragile membrane, regardless of the concentration. This film was, however, resistant to water droplets. Films prepared using Cyrene and Polarclean were placed in an oven heated to 58 °C and 78 °C respectively and left overnight to ensure the removal of any residual solvent. This additional step was necessary due to the lower volatility of these solvents compared to halogenated solvents, whose boiling points at atmospheric pressure are significantly lower (40 °C for dichloromethane, 61 °C for chloroform, 226 °C for Cyrene, and 280 °C for Polarclean). The last solvent tested was dichloromethane, which resulted in the preparation of a homogenous film with good adhesion and resistance to water penetration, while also remained stable during basic handling.

As the thickness of the film plays an important role in the detection of hydrocarbons (due to the penetration depth of the evanescent wave), a reliable coating method capable of producing reproducible thin films had to be established. Two methods of functionalization were evaluated: spin-coating and knife-coating.

The deposition of the PHA solution requires heating the substrate just below the solubilization temperature (Table 2) beforehand, so that halogenated solvents have time to form a homogenous layer of solution on top (and not cause imperfections in the structure of the film). In the case of Polarclean and Cyrene, the film jellifies if the substrate's temperature is too low. For this reason, the spin-coating method proved to be problematic as the machine and other equipment could not be reliably maintained at the required temperatures. While this method proved to be usable, under these conditions it was not reliable to produce films with consistent properties. The knife-coater, however, enabled the maintenance of a consistent temperature for all of the used equipment and substrates, making it the preferred technique for preparing films for further testing.

As the main objective of this study was to seek the possibility of using PHAs as a coating material for BTX detection using MIR sensors, the best solvent—dichloromethane—was selected for the rest of the study. However, the results obtained suggest that green solvents such as Cyrene or Polarclean could potentially be used for this application after further optimization (which lies outside of the scope of this study). In particular, membrane formation by phase inversion induced by precipitation in a non-solvent bath (instead of solvent evaporation) should be investigated.<sup>27</sup>

For the remainder of the study, PHAs other than P3HB3HV were considered. In all cases, dichloromethane was used as the solvent and knife-coating was applied as the casting technique. All of the tested polymers behaved the same during the solution's preparation, a notable exception being P3HB4HB, which took around 60 min to dissolve. In addition, PHO was used as a 20% w/w dichloromethane solution due to its very low viscosity at 10% w/w, making it unsuitable for the knife-coating method.

### Characterization of the prepared membranes

The detection and quantification of pollutants using the PHA-functionalized MIR sensor developed in this study relies on the sorption and diffusion of the target molecules into the PHA-based polymeric layer, while minimizing water penetration. To evaluate the suitability of different PHA types for this application, both the physicochemical and structural properties of the polymers and films were analysed.

The morphologies of the PHA membranes deposited on sputtered Ge–Sb–Se chalcogenide thin films (which were deposited on 2" silicon wafer) were analysed by SEM at room temperature, which was used as the working environment. The objective was to evaluate the adhesion of the membrane on the chalcogenide thin films and to determine the morphology of the membrane's cross-section. Fig. 2 shows the cross-sectional views of the four membranes prepared from four PHA polymers. For all tested polymers, the absence of air bubbles at the interface between the chalcogenide glass and the polymeric membrane indicated a good adhesion of the membrane to the support. In addition, all membranes exhibited a homogeneous and dense structure, with no macrovoids observed within the polymer's structure. These are key factors in preventing water transport by convective flow through the membrane, which could compromise the analyte detection by ATR-FTIR spectrometry. It was also observed from macroscopic observations that P3HB3HV and P3HB3HH films were more prone to damage and easier to peel, making the manipulation harder in comparison with P3HB4HB and PHO membranes, which demonstrated better durability and adherence.

In addition to the cross-sectional structure of the membrane, surface properties are of key importance as they govern the interaction between the analysed fluid and the

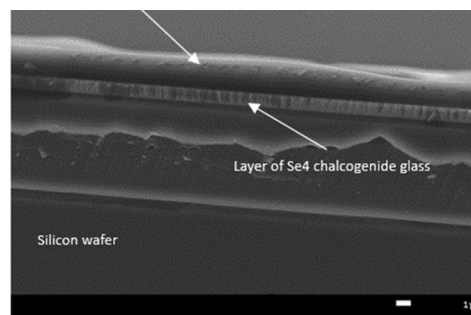


Fig. 2 SEM micrograph of (a) P3HB4HB, (b) PH3HB3HV, (c) P3HB3HH and (d) PHO film deposited on a chalcogenide glass film on a silicon wafer.



sensor material. The sorption behaviour of a specific molecule is determined by the interactions among solutes, solvents and the polymer. Specifically, the amount of the compound dissolved in the polymer membrane depends on its distribution between the solvent (water in this study) and the polymer, expressed by the partition coefficient ( $K$ ), which is defined as the ratio of the equilibrium concentration of the solute in the film to that in solution. In the present application, the sorption and diffusion of the BTX molecules into the PHA-based membranes are vital but so are the interactions between water and the PHAs. Efficient BTX detection by the MIR sensor may be compromised by water diffusion into the polymer, necessitating selective BTX/water sorption within the PHA layer. To evaluate these properties, the hydrophobicity of the PHA films was analysed using water contact angle measurements. Notably, this parameter reflects not only the inherent hydrophilicity or hydrophobicity of the material but also the surface microstructure, particularly for dense, rough surfaces with root mean squared roughness values exceeding 50–80 nm.<sup>37–39</sup> Therefore, both contact angle measurements and surface roughness analysis *via* AFM were conducted.

AFM analysis (Fig. 3) was conducted to examine the surface of the films deposited on silicon wafers *via* knife-coating under the same operating conditions as for the films prepared on ZnSe prisms. Measurements were performed on  $10\ \mu\text{m} \times 10\ \mu\text{m}$  and  $5\ \mu\text{m} \times 5\ \mu\text{m}$  areas at three different locations. P3HB3HH proved to have the roughest surface, with a root mean square (RMS) calculated by polynomial two at  $49 \pm 1\ \text{nm}$ . The surface roughness of the other polymers was calculated to be  $42 \pm 1\ \text{nm}$  for P3HB3HV,  $35 \pm 5\ \text{nm}$  for P3HB4HB and  $12 \pm 2\ \text{nm}$  for PHO. These values, being lower than the 50–80 nm range, suggest that the contact angle values could be considered as a representative of the intrinsic polymer properties.<sup>37,38</sup> These results confirmed the superior hydrophobicity of PHO compared to that of the other PHAs, making it a promising candidate for MIR sensor functionalization for the targeted application.

After sorption to the PHA membrane, the targeted molecules must diffuse through the polymer layer to be detected by ATR-FTIR. As polymer crystallinity is known to affect solute diffusion in the polymer films, the PHA crystallinity degree was determined by DSC. Most of the PHAs considered in this study were found to be semi-crystalline. This semi-crystalline structure provides a balance of properties between purely crystalline and purely amorphous materials, resulting in a strong, flexible structure with unique optical characteristics. The polymers exhibited a variety of crystallinity percentages (Table 3). This variation in crystallinity can be attributed to the differing chemical structures of the PHAs. As solute diffusion through the polymer films occurs almost exclusively through the amorphous phase of the semi-crystalline polymer films, P3HB4HB was found to be the most favourable PHA for diffusive transport.<sup>40</sup>

The ATR-FTIR spectra of the PHA membranes confirmed the absence of water in all samples, as IR absorbance bands related to water or hydroxyls group were not observed in the  $3000\text{--}4000\ \text{cm}^{-1}$  wavenumber region. Many previous studies have reported distinct IR (and Raman) band shifts resulting from

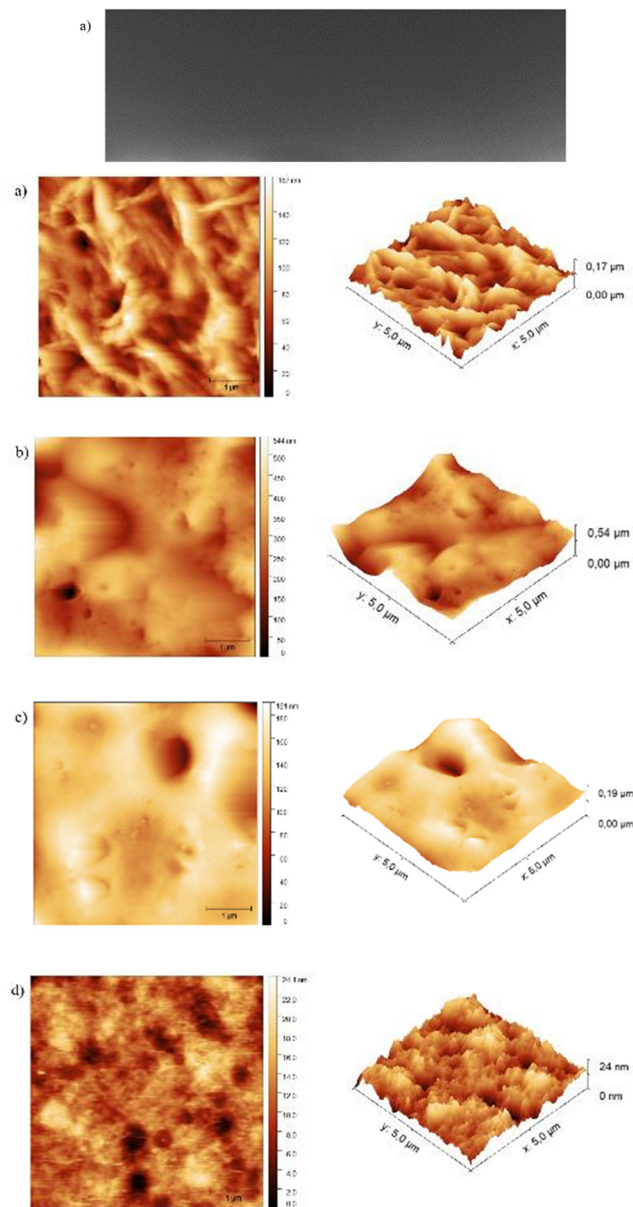


Fig. 3 AFM scan of a  $5\ \mu\text{m} \times 5\ \mu\text{m}$  area of (a) P3HB3HV film, (b) P3HB3HH film, (c) P3HB4HB film and (d) PHO film prepared by knife coating on a silicon wafer.

relatively strong  $\text{C-H} \cdots \text{O}=\text{C}$  interactions between  $\text{CH}_3$  and  $\text{C}=\text{O}$  groups, as well as from the symmetric and asymmetric stretching modes of  $\text{CH}_2$  and  $\text{CH}_3$  groups engaged in  $\text{C-H} \cdots \text{O}$  hydrogen bonding.<sup>41–43</sup> These shifts typically occur at low frequencies (below  $10\ \text{cm}^{-1}$ ) and can be influenced by the polymer's crystallinity and temperature. The IR spectra of the PHA membranes demonstrate this phenomenon, as observed when comparing the spectra obtained for the P3HB polymers. This behaviour has the potential to influence any IR measurements performed with these polymers, including those of aqueous solutions, as the analyte interacts with the polymer and has to be considered when performing IR analysis.



### ATR-FTIR measurement of the BTX molecules

As previously stated, the aim of this study was to assess the PHA polymers for their potential to form a membrane on top of an optical chalcogenide waveguide, facilitating the extraction of pollutants from water for subsequent quantification. ATR-FTIR spectroscopy based on evanescent waves has been chosen as the optimal characterisation method for accurate, non-destructive measurements of polymer efficiency for detecting pollutants in water. A study was carried out to confirm the possibility of detecting pollutants, such as BTX, to determine a concentration range for the detection and to estimate the sensitivity and resolution limits and its ability to be reused through regeneration and eventually incorporated into a microfluidic cell. The objectives of the measurements carried out by ATR-FTIR spectrometry were to determine (i) which of the tested PHAs would be the most optimal for detecting hydrocarbons in water and (ii) the dependence of their absorbance band areas on their concentration in an aqueous solution. The latter information is used to establish a calibration curve and its range of validity as a function of the concentration studied.

The suitability of the different PHA films was determined by introducing the PHA-functionalized ZnSe prism into a flow cell, which was then exposed to a flow of 50 ppm solution of BTX, flowing at a rate of 3 mL min<sup>-1</sup> at room temperature. The measurements ran for 60 min, with absorbance spectra taken every 10 min. The obtained results were then evaluated for the presence of the absorption bands representing individual BTX molecules. As seen in Fig. 4, while it was impossible to detect any hydrocarbons using P3HB3HV, small bands were observed using P3HB3HH, although their nature could not be safely determined. Conversely, P3HB4HB and PHO were both successfully used in detecting all tested hydrocarbons (Fig. 4) within

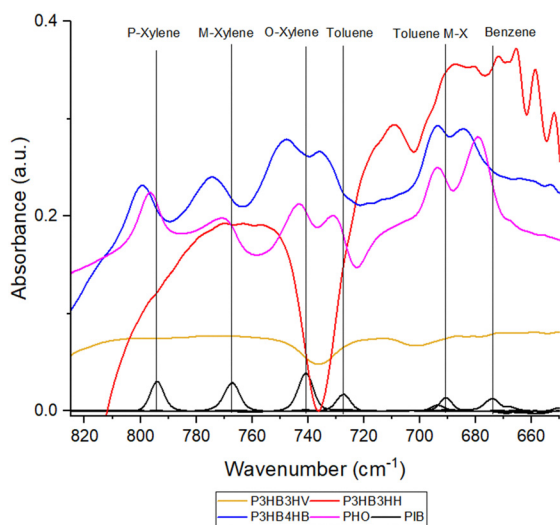


Fig. 4 The absorbance spectrum of 50 ppm BTX in water using PHA films (5  $\mu\text{m}$ ) after 60 minutes of exposure to solution and a flow rate of 3 mL min<sup>-1</sup>, compared with 5 ppm BTX solution obtained in the same conditions with 5  $\mu\text{m}$  (polyisobutylene film), showing the shift in the position of the absorbance bands (PHA films were fabricated by knife-coating, and PIB film by spin-coating).

the first (650–900 cm<sup>-1</sup>) and third (1450–1650 cm<sup>-1</sup>) infrared regions. While the last region (950–1200 cm<sup>-1</sup>), where BTX compounds are expected to exhibit absorption bands, also showed changes in the spectra in response to BTX solution, these bands could not be reliably quantified. The difference in absorption band areas related to the presence of BTX in the polymer film between the P3HB4HB and PHO polymers was around 15–20% in favour of PHO, when comparing measurements obtained at the saturation time (30–40 minutes for P3HB4HB and 60 minutes for PHO), with the exception of the toluene-*o*-xylene band that was smaller by 10%.

The bands obtained with PHO had a larger area under the absorption bands and were better defined. While the obtained absorption bands were smaller in comparison with traditionally used petroleum-based polymers<sup>7–9,33</sup> (four times when compared to the results obtained with 5- $\mu\text{m}$  polyisobutylene film under the same conditions), these results did prove, for the first time, that PHAs can be used as membranes for IR detection by means of evanescent wave spectroscopy.

These results have shown direct connections between the physicochemical properties of the used PHAs and their ability to extract molecules of the tested hydrocarbons from water. In particular, the PHA film suitability was directly linked to its crystallinity. When using the most crystalline PHA—P3HB3HV (crystallinity degree of 43%)—it was not possible to detect any BTX molecules. In contrast, BTX were detected with the three other types of PHAs with lower crystallinity degree. Using P3HB3HH (crystallinity degree of 27%), the BTX molecules were detected, but only very weak signals were obtained using 50 ppm BTX solution. Conversely, the least crystalline polymer—PHO (19%), and the amorphous polymer, P3HB4HB (0%), successfully detected BTX molecules in water (Fig. 5). It appears that higher structural order in the polymer makes it significantly harder for the molecules to diffuse in the PHA matrix. This can be explained by the fact that diffusive solute transport mostly takes place through the amorphous phase, with the crystalline phase being virtually impermeable leading to an exponential decrease in solute flux with increasing crystallinity.<sup>40,44</sup>

Moreover, under the tested conditions, the ability to detect BTX appeared to have little correlation with the hydrophobicity of the PHA-based membrane. This was evident in the case of P3HB3HH and P3HB4HB, which have similar contact angle values ( $76 \pm 1^\circ$  and  $79 \pm 3^\circ$  respectively), yet the amorphous P3HB4HB achieved a higher detection efficiency compared to the semi-crystalline P3HB3HH (crystallinity of 27%). In addition, the most hydrophobic, semi-crystalline membrane, made of PHO (contact angle of  $102 \pm 1^\circ$ , crystallinity of 19%), exhibited the best results regarding the quality of the obtained absorbance bands (the best defined peaks from the tested samples) but took longer to reach saturation. For the PHA tested in this study, having contact angle values ranging from  $67 \pm 3^\circ$  to  $102 \pm 1^\circ$ , these results underline the dominant role of crystallinity, thus making the most crystalline PHAs tested here undesirable for the present application.

As shown in Fig. 4, a low-frequency shift of 3–10 cm<sup>-1</sup> is observed in the measurements performed with P3HB4HB and



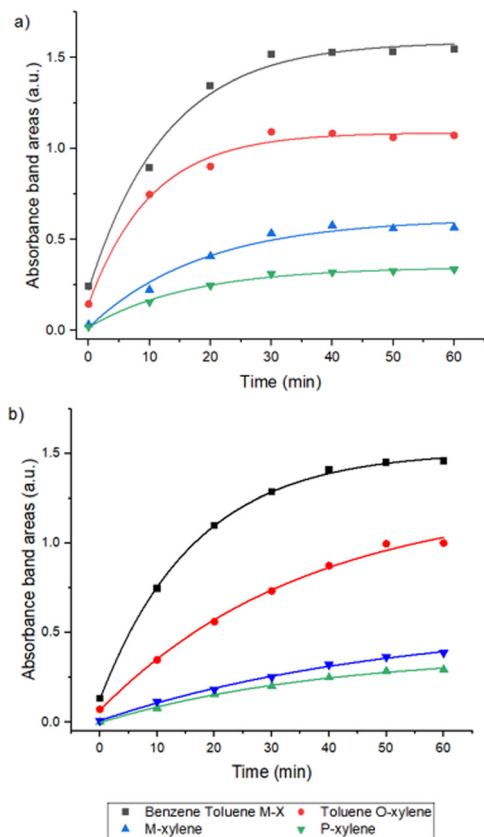


Fig. 5 Dependence of the IR absorbance band area on time using 5  $\mu\text{m}$  (a) P3HB4HB and (b) PHO polymer films to analyse 50 ppm BTX solution at a flow rate of 3  $\text{mL min}^{-1}$ .

PHO films, relative to the wavenumber values reported in the literature.<sup>8,9,33</sup> This shift was observed for all measurements and remained consistent under the same conditions. This phenomenon can be attributed to the influence of strong hydrogen bonds and stretching methyl modes, as discussed above. When compared, P3HB4HB exhibited larger shifts in the absorption band positions, ranging from 5 to 10  $\text{cm}^{-1}$ , depending on the molecule. PHO shows smaller shifts, ranging from 2 to 5  $\text{cm}^{-1}$ . These shifts were calculated based on previous measurements done with polyisobutylene.<sup>36</sup> While this phenomenon has to be considered, it influences only the positions of the bands and should not alter the magnitude of the signal.

Further experiments to quantitatively evaluate the suitability of PHAs for BTX IR sensing were carried out with P3HB4HB and PHO only. The first objective was to confirm that the temporal response of the BTX-related absorbance bands followed an expected dependence on the concentration of the solutions. Second, this dependence of the absorbance band was studied in the concentration range of 0–100 ppm of the BTX solutions. Finally, regeneration of the PHA films was studied to establish IR sensor reusability.

Fig. 5 shows the temporal variation of individual BTX-related bands for P3HB4HB and PHO membranes with individual measurements taken every 10 min until the polymer reached maximum saturation. Because the absorption bands

representing benzene/toluene M-X and toluene/o-xylene are close together, it is difficult to distinguish them, as they contribute to the appearance of a larger band. For this reason, those absorbance bands were described as one in the measurements. In the case of P3HB4HB, it took around 30–40 minutes to reach plateaus for all analytes, while PHO needed 60 min (Fig. 5). This bodes well in comparison with petroleum-based polymers, where for example the 5- $\mu\text{m}$  thick polyisobutylene film, under the same conditions, needed 80–90 minutes to reach the plateau phase (albeit showing stronger – more than 350% on average – and better-defined bands in all regions of interest).<sup>33,36</sup> These results indicate that the P3HB4HB-based sensor exhibits a faster response time compared to the PHO-based sensor, with both demonstrating quicker response times than sensors based on petroleum-based polymers. Interestingly, for both P3HB4HB and PHO, only minor differences were observed in the saturation time for each individual molecule in the mixture, suggesting that the size/structure of the molecules had little influence on the diffusion rate for these particular polymers.

Fig. 6 shows the variation of the absorption band areas at saturation (plateau reached) in the concentration range 0–100 ppm. For all studied molecules, the data can be effectively fitted with a linear model, as the coefficient of determination is generally above 0.95, promising easy calibration of the sensor, should PHAs be applied. Linear calibration also allowed the estimation of the sensitivity associated with these polymers and the detected molecules. The values of the slope coefficient of the affine functions are very similar for both polymers and are also relatively close to those observed for polyisobutylene,<sup>33</sup> ranging from 0.005 to 0.029. However, for individual molecules, the decrease in sensor sensitivity when switching from polyisobutylene to PHA is about half to two-thirds. Although these values suggest a lower overall sensitivity, this is still a positive result, as polyisobutylene has previously demonstrated reliable BTX detection at low concentrations with high resolution, while PHA polymers have intrinsic properties that make them attractive for the development of environmental optical sensors.<sup>33</sup> The theoretical limit of detection was also calculated for PHAs to be 25–130 ppb (depending on the molecule and polymer), which would make them comparable to other petrol-based polymers.<sup>36</sup> While an absorbance band could be obtained for a 5-ppm concentration of BTX, the quantification of the absorption band became difficult. Because of that, the limit of detection (LOD) for this setup was set to 5 ppm, and limit of quantification (LOQ) to 10 ppm, for detecting BTX molecules in water using P3HB4HB or PHO-functionalized IR chalcogenide prisms for ATR-FTIR spectrometry.

The kinetics associated with the detection were evaluated by considering the temporal evolution of the IR signal as a function of the hydrocarbon concentration. Four concentrations of BTX solution (10, 20, 30, and 50 ppm) were selected, and the time periods necessary to reach 30% ( $T_{30}$ ), 63% ( $T_{63}$ ), 90% ( $T_{90}$ ) and 95% ( $T_{95}$ ) of the maximum absorbance, using 5  $\mu\text{m}$  PHA films, were established. The absorption bands of benzene/toluene M-X and *p*-xylene were selected as the focus of this study, as they can be directly compared with previous



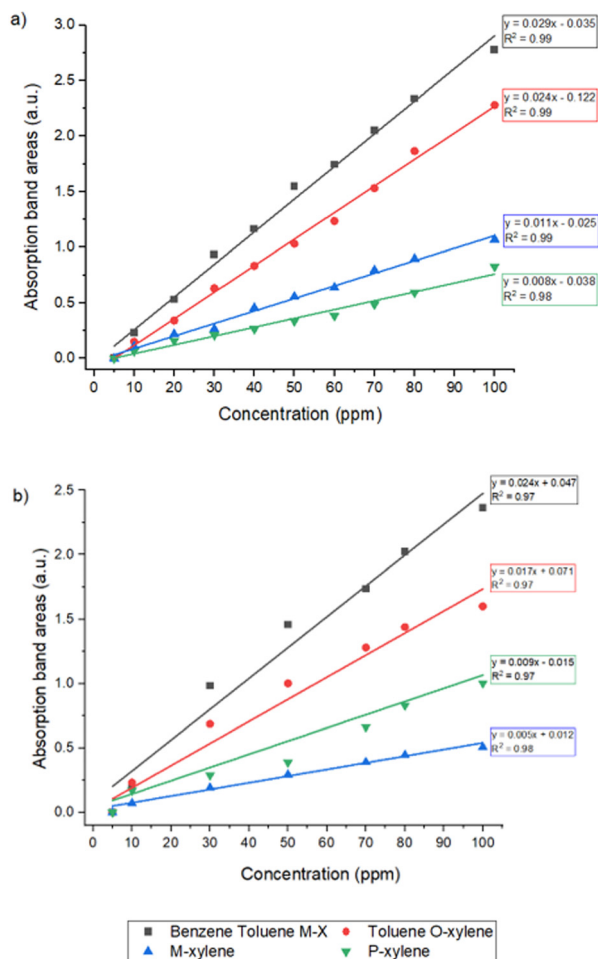


Fig. 6 Dependence of the absorbance band areas on concentration after 60 minutes of exposition using 5  $\mu\text{m}$  film: (a) P3HB4HB and (b) PHO.

measurements conducted under the same conditions using more commonly employed polymers. These previous measurements established that the bands of benzene and toluene show similar behavior, which differs notably from that of xylene bands.<sup>36</sup> The results of the present study are presented in Fig. 7.

The times required to reach these signal values depend not only on the molecule chosen but also on the concentration itself. As shown in Fig. 7, for benzene/toluene, these times start at lower values for both polymers, after which they gradually increase, with P3HB4HB showing a faster climb rate. For xylenes, this trend is very similar, although the times are generally higher than those for benzene/toluene M-X. Generally, these values are rapidly attained for benzene and toluene than for xylenes.

The  $T_{95}/T_{63}$  ratio was also calculated to assess whether it approached a value of three, which would indicate linear time dependence. This was observed in P3HB4HB for both tested absorption bands across various concentrations. Similarly, PHO exhibited this behaviour for the benzene/toluene M-X absorption bands, but it had a lower value ( $2 \pm 0.3$ ) for *p*-xylene. In comparison, polyisobutylene tested in earlier research achieved a value of three for *p*-xylene, whereas for benzene,

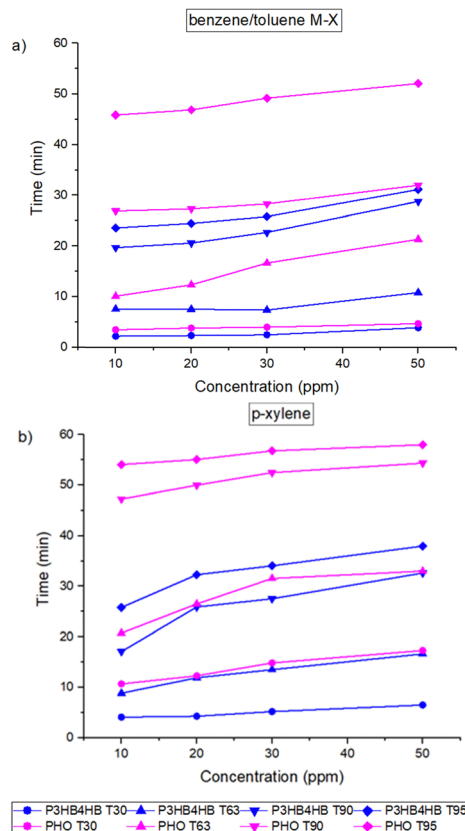


Fig. 7 Time dependence of the IR signal (at 30%, 63%, 90% and 95% of saturated signal) as a function of concentration for: (a) benzene/toluene M-X and (b) *p*-xylene using 5  $\mu\text{m}$  thick PHA films.

the ratio was higher ( $3.8 \pm 0.3$ ). These findings highlight the excellent kinetic performance of P3HB4HB, while PHO demonstrates comparable behaviour to other petroleum-based polymers.

Another important characteristic of a sensor is its reusability. While single-use sensors are recommended for certain applications, such as in health and pharmacology, they are not ideal for water quality monitoring, where reusability is crucial as it minimizes the environmental impact by promoting the longest possible life cycle of the sensor. To evaluate the reusability of PHA films, a regeneration experiment was performed for the P3HB4HB and PHO-based sensors. It consisted of a 60-minute measurement cycle followed by a 60-minute rinsing stage (regeneration cycle). During the measurement stage, the concentration of the BTX solution was kept at 50 ppm while the flow rate was adjusted to 3 mL min<sup>-1</sup>. The rinsing stage was achieved by the circulation of distilled water at room temperature at the same flow rate. Fig. 8 shows the IR spectrum of the PHO and P3HB4HB films before and after the regeneration cycle. As seen in Fig. 8, with P3HB4HB, it was possible to regenerate the film completely by a simple water rinsing at room temperature. In contrast, PHO showed the presence of residual BTX molecules, indicating incomplete regeneration, similar to polyisobutylene when tested under the same conditions.<sup>33</sup>



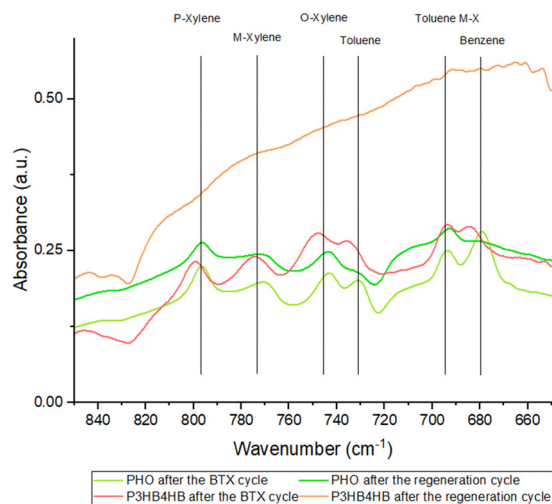


Fig. 8 The IR spectrum of the PHO and P3HB4HB film (5  $\mu\text{m}$ ) before and after the regeneration cycle for 50 ppm BTX solution (flowrate of 3  $\text{mL min}^{-1}$ ).

## Conclusions

In this study, a variety of PHA polymers were investigated as potential materials for use in ATR-FTIR-based *in situ* chalcogenide sensors dedicated to detect the pollutants present in contaminated water sources. To this aim, a PHA-based membrane was deposited on top of an infrared waveguide, ensuring extraction of pollutants from the solution as well as reducing the influence of water in the infrared spectrum. Polymers from the PHA family were chosen as an alternative to conventional fossil-based polymers because they are bio-based and offer a wide range of physicochemical properties arising from their molecular structures. Four PHAs of different molecular structure were investigated leading to comparison of different crystallinity ratios (ranging from 0% to 43%). Optimal conditions for membrane creation were found to be obtained using dichloromethane as the solvent and knife-coating as the casting technique. Physicochemical characterization showed that dense membranes without defects were formed on the chalcogenide support, exhibiting a smooth surface with slightly hydrophilic to slightly hydrophobic properties (contact angle values were in the range of 67°–102°). In this regard, PHAs proved to be compatible with chalcogenide glasses, intended for developing *in situ* sensors. Additionally, as their structure is similar to other petroleum-based polymers already tested for the detection of pollutants in water samples (e.g. polyisobutylene), the experiments were pushed further. ATR-FTIR tests revealed the key role played by crystallinity in the performance of the PHA-based MIR sensors developed. In more detail, the two most crystalline PHAs evaluated in this study (P3HB3HV and P3HB3HH) are not suitable for the targeted application, leading respectively to none and too weak BTX-related bands shown in the obtained IR spectra. In contrast, PHAs with lower crystallinity (P3HB4HB and PHO) were found to be suitable for the BTX detection and quantification. For both polymers and all molecules evaluated, the LOD was found to be 5 ppm with

the time to reach saturation in the range of 30–40 min for P3HB4HB and 60 min for PHO. The P3HB4HB film also demonstrated the ability to be regenerated using water at ambient temperature, suggesting that this film could be reused in practical applications. While the overall results of these experiments do not exceed the results obtained for traditionally used fossil-based polymers, this study reports, for the first time, the use of bio-based polymers for infrared *in situ* monitoring of chemical molecules in an aquatic environment. This opens up the possibility of using PHAs in a new field where their application is currently limited. Future studies dedicated to the fine tuning the physicochemical properties of PHA-based membranes, such as crystallinity rate and hydrophobicity, should be undertaken to further improve the sensor performance. In particular, it is important to note that the commercial-grade of PHAs used in this study were developed for other applications (e.g. packaging) and hence have not been specifically optimized for sensor functionalization. Despite this, the PHAs demonstrated promising potential as a bio-based solution for MIR spectroscopy in aquatic environments.

## Author contributions

Martin Vrážel: investigation, methodology, formal analysis, writing – original draft, review & editing; Duc Trung Tran: investigation, methodology, writing – review & editing; Patrick Loulergue: supervision, writing – review & editing; Anthony Szymczyk: supervision, writing – review & editing; Radwan Chahal: investigation supervision; Anthony Courtois: resources, writing – review; Marek Bouška: supervision; Joel Charrier: methodology; Petr Němec & Virginie Nazabal: conceptualization, funding acquisition, supervision, formal analysis, writing – review & editing.

## Conflicts of interest

There are no conflicts to declare.

## Data availability

All the data in this article are available on the secure cloud (Directory: Article PHA – Martin Vrazel – 2024) of the Information Systems Department (DSI) of the University of Rennes. The right to recover the data can be exercised without difficulty following an official request to the DSI.

## Acknowledgements

The authors would like to acknowledge ANR AQUAE (ANR-21-CE04-0011-04) project of French National Research Agency (ANR), IBAIA (101092723) Horizon Europe project, project No. 22-05179S of Czech Science Foundation (GA ČR) and CNRS Chimie (BioPHARMem project) for the financial support.



## References

- 1 J. C. G. Sousa, A. R. Ribeiro, M. O. Barbosa, M. F. R. Pereira and A. M. T. Silva, A review on environmental monitoring of water organic pollutants identified by EU guidelines, *J. Hazard. Mater.*, 2018, **344**, 146–162.
- 2 O. Ogebeide, I. Tongo and L. Ezemonye, Risk assessment of agricultural pesticides in water, sediment, and fish from Owan River, Edo State, Nigeria, *Environ. Monit. Assess.*, 2015, **187**(10), 654.
- 3 M. Alahi and S. C. Mukhopadhyay, Detection methods of Nitrate in water: A Review, *Sens. Actuators, A*, 2018, 280.
- 4 M. Alahi and S. C. Mukhopadhyay, Smart nitrate sensor: Internet of Things enabled real-time water quality monitoring, *Smart Sensors, Measurement and Instrumentation*, Springer, Cham, 2019, DOI: [10.1007/978-3-030-20095-4\\_1](https://doi.org/10.1007/978-3-030-20095-4_1).
- 5 C. Kratz, A. Furchner, G. Sun, J. Rappich and K. Hinrichs, Sensing and structure analysis by in situ IR spectroscopy: from mL flow cells to microfluidic applications, *J. Phys.: Condens. Matter*, 2020, **32**(39), 393002.
- 6 *Opportunities for photonic integrated circuits in optical gas sensors*, – IOPscience [online]. [cited 2024 Feb 16]. Available from: <https://iopscience.iop.org/article/10.1088/2515-7647/ab6742>.
- 7 C. Heath, B. Pejcic and M. Myers, Block Copolymer-Coated ATR-FTIR Spectroscopic Sensors for Monitoring Hydrocarbons in Aquatic Environments at High Temperature and Pressure, *ACS Appl. Polym. Mater.*, 2019, **1**, 21749–22156.
- 8 R. Stach, B. Pejcic, E. Crooke, M. Myers and B. Mizaikoff, Mid-Infrared Spectroscopic Method for the Identification and Quantification of Dissolved Oil Components in Marine Environments, *Anal. Chem.*, 2015, **87**, 12306–12312.
- 9 M. Baillieul, E. Baudet, K. Michel, J. Moreau, P. Němec, K. Boukerma, F. Colas, J. Charrier, B. Bureau and E. Rinnert, *et al.*, Toward Chalcogenide Platform Infrared Sensor Dedicated to the In Situ Detection of Aromatic Hydrocarbons in Natural Waters via an Attenuated Total Reflection Spectroscopy Study, *Sensors*, 2021, **21**, 2449.
- 10 A. M. Nightingale, S. Hassan, B. M. Warren, K. Makris, G. W. H. Evans and E. Papadopoulou, *et al.*, A Droplet Microfluidic-Based Sensor for Simultaneous in Situ Monitoring of Nitrate and Nitrite in Natural Waters, *Environ. Sci. Technol.*, 2019, **53**(16), 9677–9685.
- 11 B. Mizaikoff, Waveguide-enhanced mid-infrared chem/bio sensors, *Chem. Soc. Rev.*, 2013, **42**(22), 8683–8699.
- 12 U.S. Department of Health and Human Services. Interaction profile for: Benzene, Toluene, Ethylbenzene, and Xylenes (BTEX). GPO, 2004.
- 13 A. Masih, A. S. Lall, A. Taneja and R. Singhvi, Exposure levels and health risk assessment of ambient BTX at urban and rural environments of a terai region of northern India, *Environ. Pollut.*, 2018, **242**, 1678–1683.
- 14 T. Schädle, B. Pejcic and B. Mizaikoff, Monitoring dissolved carbon dioxide and methane in brine environments at high pressure using IR-ATR spectroscopy, *Anal. Methods*, 2016, **8**(4), 756–762.
- 15 A. Femenias, *et al.*, Portable tunable interband cascade laser spectrometer using thin-film waveguides for food contaminant analysis, *AIP Adv.*, 2024, **14**, 12.
- 16 R. Gabriela Flores, *et al.*, Recent advances and trends in mid-infrared chem/bio sensors, *TrAC, Trends Anal. Chem.*, 2024, 117916.
- 17 S. Meziani, *Développement de capteurs spectroscopiques en photonique intégrée dans le moyen infrarouge*, Doctoral Thesis, University of Rennes, 2024.
- 18 M. J. David, *et al.*, Chalcogenide glass thin-film and fiber structures for chemical and biological sensing, *Amorphous Chalcogenides*, 2014, 203–250.
- 19 R. Sehgal and R. Gupta, Polyhydroxyalkanoate and its efficient production: an eco-friendly approach towards development, *3 Biotechnol.*, 2020, **10**(12), 549.
- 20 V. Kalia, S. Patel and J. Lee, Exploiting Polyhydroxyalkanoates for Biomedical Applications, *Polymers*, 2023, **15**(8), 1937.
- 21 A. Steinbüchel and S. Hein, Biochemical and molecular basis of microbial synthesis of polyhydroxyalkanoates in microorganisms, *Biopolyesters*, 2001, 81–123.
- 22 R. A. Verlinden, *et al.*, Bacterial synthesis of biodegradable polyhydroxyalkanoates, *J. Appl. Microbiol.*, 2007, **102**(6), 1437–1449.
- 23 S. Modi, K. Koelling and Y. Vodovotz, Assessment of PHB with varying hydroxyvalerate content for potential packaging applications, *Eur. Polym. J.*, 2011, **47**(2), 179–186.
- 24 Y. Corre, *et al.*, Morphology and functional properties of commercial polyhydroxyalkanoates: a comprehensive and comparative study, *Polym. Test.*, 2012, **31**(2), 226–235.
- 25 A. Samrot, *et al.*, The Synthesis, Characterization and Applications of Polyhydroxyalkanoates (PHAs) and PHA-Based Nanoparticles, *Polymers*, 2021, **13**(9), 3302.
- 26 T. Pacôme, P. Loulergue, L. Paugam and J. Audic, Polyhydroxyalkanoates (PHAs) for the Fabrication of Filtration Membranes, *Membrane Technology Enhancement for Environmental Protection and Sustainable Industrial Growth*, Springer, 2021, pp. 177–195.
- 27 T. Pacôme, F. Russo, F. Galiano, P. Loulergue, S. Salerno, L. Paugam, J. Audic, L. Bartolo and A. Figoli, Sustainable fabrication and pervaporation application of bio-based membranes: combining a polyhydroxyalkanoate (PHA) as biopolymer and Cyrene™ as green solvent, *J. Membr. Sci.*, 2021, 643.
- 28 A. Teuber, *et al.*, Thin-Film Waveguide Laser Spectroscopy: A Novel Platform for Bacterial Analysis, *Anal. Chem.*, 2023, **95**(45), 16600–16608.
- 29 R. Saji, *et al.*, Application of FTIR spectroscopy in dairy products: a systematic review, *Food Humanity*, 2024, **2**, 100239.
- 30 F. Tugrul, *et al.*, A biospectroscopic approach toward colorectal cancer diagnosis from bodily fluid samples via ATR-MIR spectroscopy combined with multivariate data analysis, *Spectrochim. Acta, Part A*, 2024, **304**, 123342.
- 31 C. Vigano, J. Ruyschaert and E. Goormaghtigh, Sensor applications of attenuated total reflection infrared spectroscopy, *Talanta*, 2005, **65**(5), 1132–1142.
- 32 P. Linstrom and W. G. Mallard, Evaluated Infrared Reference Spectra in NIST Chemistry WebBook, NIST Standard



- Reference Database Number 69. [cited 2024 Feb 8] Coblenz Society, Inc. National Institute of Standards and Technology, Gaithersburg MD, 20899.
- 33 M. Baillieul, *Capteurs infrarouges de polluants aquatiques: synthèse, optimisation et qualification*, Doctoral Thesis, University of Rennes, 2018.
- 34 A. V. Bagdadi, *et al.*, Poly(3-hydroxyoctanoate), a promising new material for cardiac tissue engineering, *J. Tissue Eng. Regen. Med.*, 2018, **12**(1), e495–e512.
- 35 G. A. Ryltseva, A. E. Dudaev, N. G. Menzyanova, T. G. Volova, N. A. Alexandrushkina, A. Y. Efimenko and E. I. Shishatskaya, Influence of PHA Substrate Surface Characteristics on the Functional State of Endothelial Cells, *J. Funct. Biomater.*, 2023, **14**(2), 85.
- 36 M. Vrážel, *et al.*, Surface functionalization of a chalcogenide IR photonic sensor by means of a polymer membrane for water pollution remediation, *Analyst*, 2024, **149**(18), 4723–4735.
- 37 M. F. Ismail, B. Khorshidi and M. Sadrzadeh, New insights into the impact of nanoscale surface heterogeneity on the wettability of polymeric membranes, *J. Membr. Sci.*, 2019, **590**, 117270.
- 38 R. S. Hebbbar, A. M. Isloor and A. F. Ismail, *Contact angle measurements. Membrane characterization*, Elsevier, 2017, pp. 219–255.
- 39 M. F. Ismail, M. A. Islam, B. Khorshidi, A. Tehrani-Bagha and M. Sadrzadeh, Surface characterization of thin-film composite membranes using contact angle technique: review of quantification strategies and applications, *Adv. Colloid Interface Sci.*, 2022, **299**, 102524.
- 40 A. Peterlin, Dependence of diffusive transport on morphology of crystalline polymers, *J. Macromol. Sci., Part B: Phys.*, 1975, **11**(1), 57–87.
- 41 K. Papchenko, M. Degli Esposti, M. Minelli, P. Fabbri, D. Morselli and M. G. De Angelis, New sustainable routes for gas separation membranes: the properties of poly(hydroxybutyrate-co-hydroxyvalerate) cast from green solvents, *J. Membr. Sci.*, 2022, **660**, 120847.
- 42 H. Wang and K. Tashiro, Reinvestigation of crystal structure and intermolecular interactions of biodegradable poly(3-hydroxybutyrate)  $\alpha$ -form and the prediction of its mechanical property, *Macromolecules*, 2016, **49**(2), 581–594.
- 43 H. Sato, Y. Ando, J. Dybal, T. Iwata, I. Noda and Y. Ozaki, Crystal Structures, Thermal Behaviors, and C–H···O=C Hydrogen Bondings of Poly(3-hydroxyvalerate) and Poly(3-hydroxybutyrate) Studied by Infrared Spectroscopy and X-ray Diffraction, *Macromolecules*, 2008, **41**(12), 4305–4312.
- 44 J. G. A. Bitter, Effect of crystallinity and swelling on the permeability and selectivity of polymer membranes, *Desalination*, 1984, **51**(1), 19–35.

